IEEE Access
Multidisciplinary | Rapid Review | Open Access Journal

Received October 30, 2018, accepted November 21, 2018, date of publication November 27, 2018,
date of current version December 27, 2018.

Digital Object Identifier 10.1109/ACCESS.2018.2883486

Wireless Power Transfer Using an RF Plasma

LOUIS WY LIU[1,2], ABHISHEK KANDWAL[3], HONGJIAN SHI[1], AND QINGSHA S. CHENG[1]

[1]Department of Electrical and Electronics Engineering, Southern University of Science and Technology, Shenzhen, China
[2]Faculty of Engineering, Vietnamese-German University, Thu Dau Mot, Vietnam
[3]Shenzhen Institutes of Advanced Technology, Chinese Academy of Sciences, Shenzhen, China

Corresponding author: Louis Wy Liu (planetx4u@yahoo.com)

This work was supported in part by the National Natural Science Foundation of China under Grant 61471258 and in part by the Peacock Technology Innovation under Grant KQJSCX20170328153625.

All authors contributed equally to this work.

ABSTRACT Storing the energy from an RF plasma was once believed to be difficult. Here, we demonstrate how an RF plasma can be delivered through water or air and harvested as a storable DC voltage. In this method, experiments I and II were conducted to prove the feasibilities of transmitting a power as an RF plasma through water and air. In both experiments, the RF plasma was transmitted from an USB/battery-powered RF plasma source with the help of a monopole antenna, whilst the power in the receiving end was captured using an Avramenko diode configuration and then multiplied using a multi-staged differential voltage multiplier. In both experiments, the results and efficiency of energy harvesting highly depended on the number of multiplication stages in the differential voltage multiplier. In experiment I, the RF power was successfully delivered along the surface of water as a surface wave to light up a neon lamp, with the measured transmission efficiency being stable over almost the whole transmission range. However, the transmission efficiency was weakly dependent upon the water conductivity. In experiment II, the RF power was successfully delivered through air but only over a rather limited transmission range, beyond which the approximate transmission efficiency was found to be inversely proportional to the transmission range. The Overall findings of this paper have opened up the possibility for 1) energizing wearable electronics with an RF plasma; 2) sensing of RF plasmas; and 3) harvesting electric energy of a natural plasma source such as a lightning strike over a wet land or an ocean.

INDEX TERMS Avramenko diode configuration, plasma, displacement current, electrostatic waves, plasma surface waves, lateral waves, Catatumbo lightning, wireless power transfer.

I. INTRODUCTION

Common intuition dictates that wearable electronics should be powered by batteries. However, batteries are bulky items which, when running out, have to be manually replaced or recharged using a special electric cable. The best scenario is to be able to energize these devices without replacement of batteries or to recharge them wirelessly. At the time of this writing, energizing wearable electronics is currently a major issue being researched by scientists.

One of the well-known approaches for wirelessly energizing a wearable device is by electromagnetic induction. In this approach, the device worn by the body has been mounted with a mini-coil which acts as a secondary coil. The skin is patched with another coil which acts as the primary coil. The electric current passing through the primary coil produces a magnetic field which induces another electric current in the mini-coil by magnetic coupling. The wearable device has to be very close to the primary coil on the skin because the magnetic field generated this way decays exponentially with distance from the primary coil. According to the Stanford group [1], who is a pioneer of wireless power transfer by magnetic coupling, the transmission efficiency with this approach is 0.1%.

In another approach [2], a wearable device is powered by radio waves. Radio waves tend to dissipate as they pass through the body. To overcome this problem, an array of antennas is used to generate a group of radio waves of slightly different frequencies. These radio waves overlap and combine in different manners as they propagate. At certain points, where these radio waves interfere constructively with each other, they provide enough energy to energize an implanted or wearable device. At the time of this writing, the efficiency as reported in [2] is -47 dB over a distance of 6cm.

According to our experience, wireless power transfer with radio waves or magnetic coupled waves is a sound technique but there are always situations where a much higher harvested power is warranted. To overcome this issue, we propose the use of RF plasma to charge up or to energize a wearable device wirelessly. Among all forms of energy which have

been considered in the published literature, electric plasmas in KHz or MHz ranges are one of the few options which allow a large amount of the electric energy to be cost-effectively delivered as a ground wave without harmful effects to human [3], [4]. In an article authored by Nikola Tesla [3], he has proven beyond any doubt that powerful high frequency electrical discharges of several hundred thousand volts could be passed through the human body to operate a dynamo without inconvenience or hurtful consequences. Electric plasmas have been similarly used by Marconi [5] in his prize winning experiments without harming the environment.

High frequency electricity such as an RF plasma is known to be substantially less lethal than lower frequency electricity because, when the frequency is sufficiently high, the electric energy will propagate as a surface wave or radiate out as a radiation loss. While conducting a high voltage experiment at a high frequency appears to be dangerous, many people have attested the opposite by their own experience [6], [7].

Energizing wearable electronic devices is one of the goals of this work. However, the main objectives of this work is to extend the proposed method for the following applications: 1) wireless sensing of an RF plasma; 2) capturing electricity from a natural plasma source such as a lightning strike from the sky. At the time of this writing, there have been some research efforts devoted to closed-circuit approaches of sensing of an RF plasma but harvesting lightning energy is one of the most misunderstood technologies [8]. Despite all the negative rumors, there have been several attempts to harvest lightning energy since 1980s. There has not been any serious attempt to improve the methodology in part because it is difficult to predict precisely where a lightning bolt is going to strike on a dry land. On the other hand, storing energy from a high voltage electric discharge has been erroneously thought to be very difficult, if not impossible. However, an ocean or a wet land is a completely different story in some areas of the world [9]–[11]. Given a technology which can capture electric surface waves, there is no reason to believe that it is impossible to harvest or store this surface energy as a result of a lightning strike on an ocean, lake or river.

II. TRANSMITTING ENERGY VIA RF SURFACE PLASMA WAVES

Water is a conducting material which can support propagation of plasma surface wave. When a lightning bolt strikes on an ocean, a river, a lake or even a wet land, the plasma surface wave from the lightning bolt largely spreads along the surface of the water [9]. This plasma surface wave can not only hit ships or objects that are nearby, but also electrocute marine animals close to the surface of the water. However, the fish or divers swimming at greater depths usually survive with no injury even though the salt water is highly conductive [9]. It is a known fact that the AC electricity spreads outward along the surface of the water in the form of surface waves and does not really go too deep into the water itself.

Electric plasmas are known to be able to support a particular mode of electromagnetic energy which travels on the surface [16], [17]. This energy is known as a plasma surface wave. From the plasma physics point of view, any medium with a finite conductivity can support the propagation of plasma surface waves. Contrary to the common belief that surface waves should not exist on the surface of dielectric materials, the results of our investigation strongly suggests that semiconductors or lossy dielectric materials can indeed support propagation of plasma surface waves. In a plasma surface wave, of which the voltage is in general higher than those of the conventional surface waves, the electric field oscillating in parallel with the direction of the wave propagation is normally the strongest along the air-medium interface. The strength of this oscillating electric field away from the air-medium interface is in general not significant.

Plasma surface waves are in general electrostatic in nature. In terms of Maxwell's electromagnetic physics, the said plasma surface wave is equivalent to a traverse magnetic mode with a negligible magnetic field. The oscillating electric field of plasma surface wave in parallel with the dielectric surface is normally strong enough to cause either a dielectric breakdown or a lowered surface resistivity.

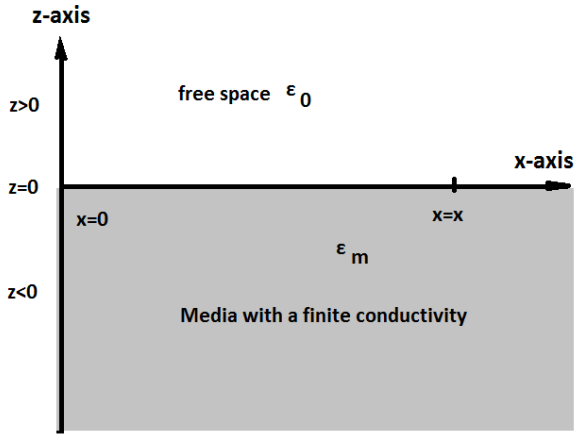

FIGURE 1. Cross-sectional view of the transmission medium that supports propagation of plasma surface wave.

Fig. 1 illustrates how the cross-sectional view of the transmission medium which supports propagation of plasma surface wave. In this work, the media with a finite conductivity is water.

In Fig. 1, at $x = 0$, the electric field in time domain is given by:

$$E\,(x = 0, t) = A\exp(-i\omega t) \tag{1.1}$$

Let's define the phase velocity of the plasma wave $v_{ph} = \omega/k_x$ where the k_x is the wave number in the propagation direction. When the propagation displacement becomes dummy in the x-direction, i.e. $x = x$, the electric field in time domain is given by:

$$E\,(x = x, t) = E\left(0, t - \frac{x}{v_{ph}}\right) = A\exp\left(-i\omega t - \frac{\omega}{v_{ph}}x\right) = A\exp(-i\omega t - k_x x) \tag{1.2}$$

Using Maxwell's equations in closed form, we obtain the following differential equations that describe the electric fields in free space as well as in the medium with a finite conductivity. For air:

$$\nabla^2 E + \frac{\omega^2}{c^2} E = 0 \tag{1.3}$$

For the medium with a finite conductivity:

$$\nabla^2 E + \frac{\omega^2}{c^2} \varepsilon_m E = 0 \tag{1.4}$$

where $\nabla^2 = \frac{\partial^2}{\partial z^2} + \frac{\partial^2}{\partial x^2} = \frac{\partial^2}{\partial z^2} - k_x^2$.

In other words, the electric field equation for the air half space is:

$$\frac{\partial^2 E_x}{\partial z^2} - (k_x^2 - \frac{\omega^2}{c^2}) E_x = 0 \tag{1.5a}$$

$$\frac{\partial^2 E_x}{\partial z^2} - \alpha_a^2 E_x = 0 \tag{1.5b}$$

where

$$\alpha_a^2 = (k_x^2 - \frac{\omega^2}{c^2}) \tag{1.5c}$$

The solution to Equation (1.5b) can be expressed as:

$$E_x = A_a \exp(\alpha_a z) \exp(-j(\omega t - k_x x)) \tag{1.5d}$$

By the same token, the electric field equation inside the medium with a finite conductivity is:

$$\frac{\partial^2 E_x}{\partial z^2} - (k_x^2 - \frac{\varepsilon_m \omega^2}{c^2}) E_x = 0 \tag{1.6a}$$

$$\frac{\partial^2 E_x}{\partial z^2} - \alpha_m^2 E_x = 0 \tag{1.6b}$$

where

$$\alpha_m^2 = (k_x^2 - \frac{\varepsilon_m \omega^2}{c^2}) \tag{1.6c}$$

The solution to Equation (1.5b) can be expressed as:

$$E_x = A_m \exp(-\alpha_m z) \exp(-j(\omega t - k_x x)) \tag{1.6d}$$

The electric field at the interface (i.e. $z = 0$) should be continuous along the vertical axis z. Substituting z = 0 into Equations (1.5c) and (4.6c), we obtain:

$$A_m = A_a \tag{1.7}$$

Using the first Maxwell's equation, which dictates that $\nabla E = 0$, we obtain:

$$\frac{\partial E_x}{\partial z} + \frac{\partial E_z}{\partial z} = 0 \tag{1.8}$$

$$\frac{\partial E_z}{\partial z} = -jk_x E_x \tag{1.9}$$

Integrating both sides of Equation (1.9), we obtain:

For z > 0:

$$E_z = \frac{jk_x}{\alpha_a} A_a \exp(\alpha_a z) \exp(-j(\omega t - k_x x)) \tag{1.10}$$

Similarly, for z < 0:

$$E_z = -\frac{jk_x}{\alpha_m} \varepsilon_m A_a \exp(-\alpha_m z) \exp(-j(\omega t - k_x x)) \tag{1.11}$$

Hence, at z = 0,

$$\frac{1}{\alpha_a} = -\frac{\varepsilon_m}{\alpha_m} \tag{1.12}$$

Equations (1.5c) and (1.6c) can be rewritten using the relation given in Equation (4.12) in the following manner:

For z = 0+,

$$\alpha_a = \frac{\omega}{c} \left(-\frac{\varepsilon_m^2}{1 + \varepsilon_m} \right)^{\frac{1}{2}} \tag{1.13}$$

For z = 0−,

$$\alpha_m = \frac{\omega}{c} \left(-\frac{1}{1 + \varepsilon_m} \right)^{\frac{1}{2}} \tag{1.14}$$

For plasma surface wave to exist along the surface, α_m must be real. From Equation (4.14), this is possible only if $1 + \varepsilon_m < 0$. In terms of plasma physics, this means:

$$1 + \varepsilon_r - \frac{\omega_p^2}{\omega^2} < 0 \tag{1.15}$$

where ε_r is the real part of permittivity of the medium with finite conductivity. ω is the frequency of the plasma wave. ω_p in Equation (1.15) is the plasma frequency of the medium with a finite conductivity, which is given by the following formula:

$$\omega_p = \sqrt{\frac{n_e e^2}{m \varepsilon_0}} \tag{1.16}$$

where n_e is the electron density of the medium with a finite conductivity, e is the electron charge, m is the electron mass and ε_0 is the permittivity of free space. From Equation (1.15), we can deduce that, in order for a plasma surface wave to exist, the following equation must be satisfied:

$$\omega < \frac{\omega_p}{\sqrt{1 + \varepsilon_r}} \tag{1.17}$$

If the medium with a finite conductivity is a plasma, $\varepsilon_r = 1$ and we have $\omega < \frac{\omega_p}{\sqrt{2}}$. In inequality (1.17), the value of the expression on the right side is collectively known as surface plasmon resonance frequency.

When $\omega \ll \omega_p$, where the plasma surface wave becomes a reality, the real part of the permittivity of the medium with a finite conductivity is basically insignificant. The imaginary part of the permittivity ε_m becomes dominant and can be expressed as:

$$\varepsilon_m \approx j \frac{\sigma}{\omega \varepsilon_0} \tag{1.18}$$

where σ is the conductivity of the medium that supports the plasma surface wave. From Equations (1.5c) and (1.6c), we can obtain the following approximation with the help of Equation (1.18):

$$\alpha_m \approx \alpha_a \sqrt{|\varepsilon_m|} \tag{1.19}$$

Equation (1.19) suggests that the strength of the evanescent electric field was negatively associated with the magnitude of the permittivity of the medium with a finite conductivity, $|\varepsilon_m|$, which, according to Equation (1.18), depends on the operating frequency. Since the evanescent electric field strength is highest in close vicinity of the surface of the dielectric material, the energy to be harvested should be as close to the surface as possible.

The plasmon frequency of water is known to be 21eV (or 8.6849 × 1015 Hz) [19]. According to the above analysis, the transmitted energy is primarily plasma surface wave. The conductivity of tap water is anywhere between 50S and 800S, which, according to Equation (1.18), giving rise to a permittivity α_m anywhere between 3.38 × 1010j and 5.41 × 1012j. According to Equations (1.19), (1.5d) and (1.6d), such a large value of imaginary part of the permittivity has one important implication: the electric field in parallel with the direction of propagation is almost absent in the water and all the energy of the plasma surface wave is concentrated at or just above the water surface.

III. HARVESTING ENERGY FROM AN RF PLASMA

The core idea of this work is to use the Avramenko diode configuration to harvest a wirelessly transmitted power [12], [13]. Avramenko diode configuration was originally intended for single-wire power transfer [24]. Single-wire power transfer means delivering a power through a conducting medium in the absence of any earth return. On the other hand, wireless power transfer means a power through a semiconducting or non-conducting medium in the absence any earth return. This wirelessly transmitted power must be an AC electricity which can be either a surface wave propagating on the surface of a conducting or dielectric material [14]–[16], a space electromagnetic wave [14], [15], an RF plasma, or a combination of these waves. Surface wave is a guided wave with a stronger oscillating electric field than that of a space electromagnetic wave. Historically, this concept has been used to an advantage to implement long range wireless power transfer by both Tesla [3], [4] and Marconi [5].

Fig. 2(a) shows the circuit topology of the proposed energy harvesting device (EHD) for harvesting energy from an RF Plasma. The circuit comprises i) an open-ended single-wire transmission line, ii) an Avramenko diode configuration [12]–[15], and iii) a differential voltage multiplier cascaded in series [12], [14], [15]. What follows describes each component of the EHD in details.

A. OPEN-ENDED SINGLE-WIRE TRANSMISSION LINE

The single-wire transmission line, as shown in Fig. 2, serves as an open-ended interfacing port for capturing the electrical energy from the RF source. It can be any piece of metal interfacing with the dielectric medium which supports the wireless propagation of the RF plasma. The geometry of the single-wire transmission line determines its characteristic impedance which should be comparable to the surface impedance of the dielectric medium.

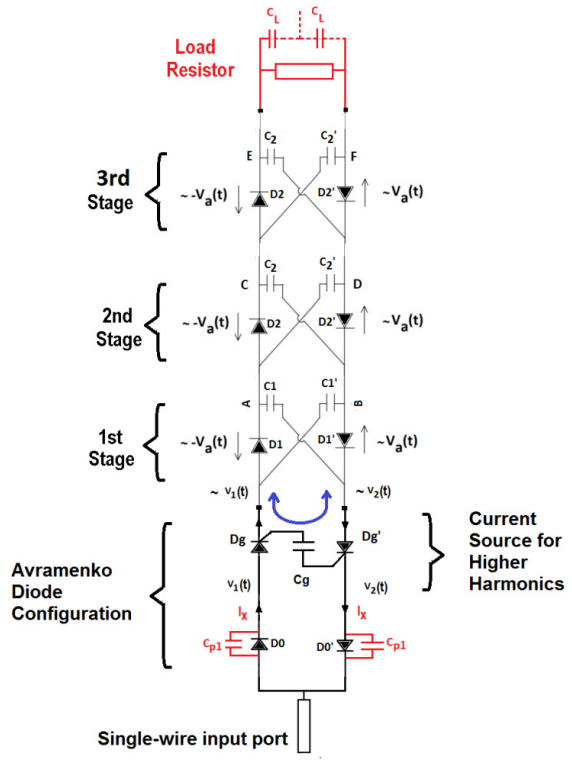

(a)

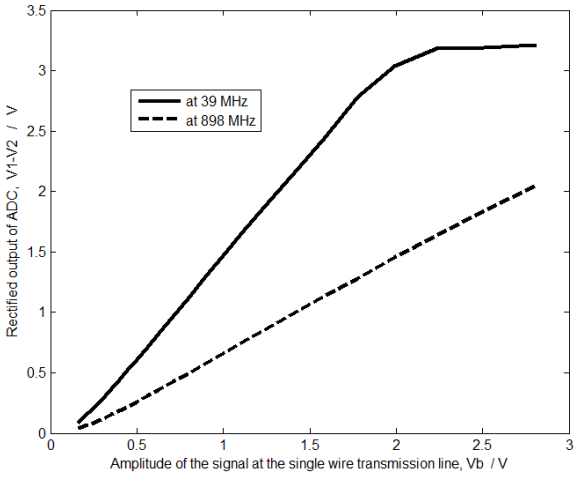

(b)

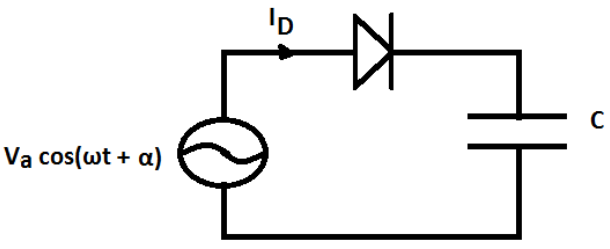

(c)

FIGURE 2. Energy harvesting device with a 3-staged differential voltage multiplier. a) The schematic diagram (the purple double arrows indicates the direction of the harmonic current); b) the measured output of the Avramenko diode configuration (V_2-V_1) as a function of the amplitude of the signal at the single wire transmission line; c) schematic of the basic building block for analysis.

B. AVRAMENKO DIODE CONFIGURATION

Before any analysis, it is important to develop an expression to compute the rectified voltage across the diode in Fig. 2(c), which is the circuit template used for the analysis of various circuit components in the EHD. The relationship between the current and voltage of a typical diode can be summarized as:

$$I = I_s\left(exp\left(\frac{V_D(t)}{V_T}\right) - 1\right) \tag{2a}$$

where V_T is the threshold voltage given by $V_T = \eta KT/q$. I_S is the reverse saturation current. η is the ideality factor depending on the quality of the diode. K, T and q are respectively the Boltmann's constant, the absolute temperature and the electron charge. $KT/q = 26mV$ at room temperature. The formula given in Equation (2a) has neglected the effect of the reverse breakdown voltage of the diode.

Using the formula given in Equation (2a), the DC voltage across the diode in Fig. 2(c) can be similarly determined according to Equation (2b):

$$C\frac{d}{dt}\left(V_a cos\left(\omega t + \alpha\right) - V_D\left(t\right)\right) = I_s\left(exp\left(\frac{V_D(t)}{V_T}\right) - 1\right) \tag{2b}$$

With some algebraic manipulation on Equation (2b), the following formula can be obtained:

$$V_D(t) \approx V_T ln\left(I_0\left[\frac{V_a}{V_T}\right]\right) + V_T ln\left(\frac{I_s}{2Cf\ V_T}\right) \tag{2c}$$

In Equation (2c), $V_D(t)$ is normally a weak function of time. The formula given in Equation (2c) will be used hereafter as a template circuit for derivation of the input/output relationship of the EHD as shown in Fig. 2(a).

Equation (2c) shows that the approximate potential difference across the diode, $V_D(t)$, is virtually independent of time, t. Due to the junction capacitance across the diode in Fig. 2(c), there may be a small amount of frequency dependent AC harmonics across the diode. For this reason, it is logical to suggest that, in Fig. 2(a), the Avramenko diode configuration (ADC) formed by diodes $D0$ and $D0'$ converts the monopole AC electricity from the single-wire transmission line to a dipole energy, which is expected to be a superimposition of a large portion of a DC voltage and a small portion of AC harmonics.

To simplify our analysis, the nonlinear junction capacitances C_{p1} and C'_{p1} are assumed to be negligible. Suppose that there is an electromagnetic energy being captured by the single-wire transmission line. The amplitude of the AC voltage at the single-wire transmission line is assumed to be V_b.

In Fig. 2(a), the thyristors D_g and D'_g, which are two identical thyristors with their gate terminals connected by capacitor. Similar to ordinary diodes, the voltage in a thyristor can be determined using Equation 2c. However, the current in thyristors D_g and D'_g, depends on the AC harmonics, of which the amplitudes should be low if the $D0$ and $D0'$ are high-speed diodes. Hence, there will not be a significant DC voltage drop across either D_g and D'_g. However, the capacitor Cg allows only AC current to flow through. Thyristors are known to have a negative dynamic resistance. Together with capacitor Cg, these negative dynamic resistances form a positive feedback loop for amplifying the AC harmonics in the circuit. Whilst there can be very limited harmonic power at $D0$ or $D0'$, there can be a large harmonic current at the load. This amplified AC harmonic current from $D0$ and $D0'$ can be used to feed the differential voltage multiplier at the next stage.

If the input impedance of the differential voltage multiplier is sufficiently high, the current I_x is close to zero, and Equation (2a) can be rewritten as:

$$C_g\frac{dV_1}{dt} = I_s\left(exp\left(\frac{V_1\left(t\right) - V_B(t)}{V_T}\right) - 1\right) \tag{2d}$$

$$-C_g\frac{dV_2}{dt} = I_s\left(exp\left(\frac{V_B\left(t\right) - V_2(t)}{V_T}\right) - 1\right) \tag{2e}$$

The rectified voltage at the output of the Avramenko diode configuration, V_2-V_1, can be algebraically manipulated by combining Equations (2a) and (2b) together and approximated by the following expression according to the formula given in Equation (2c):

$$V_1 - V_2 \approx 2V_T ln\left|1 - \frac{I_s}{2C_g f\ V_T} I_0\left[\frac{V_b}{V_T}\right]\right| \tag{2f}$$

where $I_0\left[\ldots\right]$ is the operator for zero-order modified Bessel function of the first kind, f is the operating frequency and V_b is the amplitude of the voltage at the single transmission line at the input of the Avramenko's diode configuration (ADC).

When V_b is sufficiently large, the second term inside the *ln()* function becomes much greater than *1*. Using the approximation formula for the modified Bessel function of the first kind, Equation (2f) can be further approximated as follows:

$$V_1 - V_2 \approx 2V_T ln\left|\frac{I_s}{2C_g f\ V_T}\sqrt{\frac{V_T}{2\pi V_b}} exp\left(\frac{V_b}{V_T}\right)\right| \tag{2g}$$

$$V_1 - V_2 \approx 2V_T ln\left|\frac{I_s}{2C_g f\ V_T}\sqrt{\frac{V_T}{2\pi V_b}}\right| + 2V_b \tag{2h}$$

On the right side of Equation (2h), the second term is normally much greater than the first term. When the operating frequency is sufficiently low, the effects of the junction capacitances from the diodes, C_g, C'_g, C_{p1} and C'_{p1} are normally negligible and the first term on the right side of Equation (2h) is small. In this case, the maximum rectified output of the Avramenko diode is roughly two times the amplitude of the input voltage at the single wire transmission line:

$$\max(V_1 - V_2) \approx 2V_b \tag{2ha}$$

However, if the operating frequency exceeds the UHF band, the first term on the right side of Equation (2h) will become negative, thereby reducing the rectified DC output of the Avramenko diode configuration.

The absence of the diode current term in Equation (2h) is suggestive of the fact that the voltage at the output of the

Avramenko diode configuration (V_2-V_1) is weakly dependent on the current at the single-wire input port. In other words, the Avramenko diode configuration acts as a sensor of AC electric fields, with its output V_2-V_1 being dependent mainly on the AC electric field strength.

Equation (2ha) appears to suggest that the rectified DC output of the Avramenko diode configuration (V_2-V_1) is weakly dependent of the operating frequencies. In practice, however, C_{p1} and C'_{p1} are voltage dependent and cannot be ignored at UHF frequencies or above. When the frequency reaches the UHF band, C_{p1} and C'_{p1} tend to bypass some of the high-frequency harmonics due to the nonlinearity of the diodes *D0* and *D0′*, ending up with a mixture of AC harmonics and a reduced DC voltage at the output of the Avramenko diode configuration.

Due to the presence of junction capacitances C_{p1} and C'_{p1} in the diodes of the Avramenko diode configuration, the rectified DC voltage at the output of the Avramenko diode configuration is in general negatively associated with the operating frequency. This negative association has been experimentally confirmed by our measurement as shown in Fig. 2(b). The diodes used in this measurement were a Schottky detector diode from Skyworks, SM7630-061, with a junction capacitance of $0.14pF$.

It can be observed from Fig. 2(b) that the output of the ADC is also hard limited by the reverse breakdown voltage of *D0*, or *D0′*, or both, when the output of the Avramenko diode reaches a certain voltage. In this measurement, the reverse breakdown voltages of both diodes were approximately 4.5 volts. As a result of this reverse breakdown voltage, the output of this Avramenko diode configuration has failed to exceed 3.25 volts when the operating frequency was 39MHz (See Fig. 2(b)). These reverse breakdown voltages can be used to limit the maximum output voltage, the excess of which would otherwise damage the energy harvesting device. For this reason, the energy which an ADC can capture is not necessarily a continuous wave. If diode *D0* and *D0′* can withstand a sufficiently high voltage, the energy to be captured by the proposed energy harvester can be in the form of a mega-voltage impulse.

C. DIFFERENTIAL VOLTAGE MULTIPLIER

As mentioned in the previous section, the output of the Avramenko diode configuration contains not only a DC voltage or but a small portion of AC harmonics. These AC harmonics can be further rectified to boost the output DC voltage using a differential voltage multiplier as shown in Fig. 2(a). The proposed differential voltage is a novel circuit topology that converts the AC harmonics which remain at the output of the Avramenko diode configuration into a DC voltage. The differential voltage multiplier can have a different number of multiplication stages, which in turn yield different input impedance at the differential voltage multiplier.

Suppose the amplitude of 1st harmonic at the differential output of the Avramenko diode is V_a, which is normally dependent on the nonlinearity of diodes *D0* and *D0′*as well as the characteristics of thyristors *Dg* and *Dg′*. Using the formula given in Equation (2c), the DC output after the 1st stage of multiplication V_{AB} can be expressed as:

$$V_{AB} \approx 2V_T ln\left(I_0\left[\frac{V_a}{V_T}\right]\right) + 4V_T ln\left(\frac{I_s}{2Cf\ V_T}\right) + 2V_b + V_T ln\left|\sqrt{\frac{V_T}{2\pi V_b}}\right| \quad (2i)$$

The last term on the right side of Equation (2i) is usually too small to be considered. But, Equation (2i) can be further reduced into the following form:

$$V_{AB} \approx 2V_T ln\left(I_0\left[\frac{V_a}{V_T}\right]\right) + 4V_T ln\left(\frac{I_s}{2Cf\ V_T}\right) + 2V_b \quad (2j)$$

Similarly, the DC output after the 2nd stage of multiplication V_{CD} can be expressed as:

$$V_{CD} \approx 2V_T ln\left(I_0\left[\frac{V_a}{V_T}\right]\right) + 2V_T ln\left(\frac{I_s}{2Cf\ V_T}\right) + V_{AB} \quad (2k)$$

where the V_a represents the amplitude of the 1st harmonic voltage component after the 1st stage of multiplication. Since V_a is negligible in practice because of the weakening effect of the multiplication stage, Equation (1k) can be rewritten as:

$$V_{CD} \approx 2V_T ln\left(\frac{I_s}{2Cf\ V_T}\right) + V_{AB} \quad (2l)$$

Or equivalently,

$$V_{CD} \approx 2V_T ln\left(I_0\left[\frac{V_a}{V_T}\right]\right) + 6V_T ln\left(\frac{I_s}{2Cf\ V_T}\right) + 2V_b \quad (2m)$$

Equations (2j) and (2m) suggest that the EHD tends to operate favourably when the operating frequency satisfies the following condition:

$$f < \frac{I_s}{2CV_T} \quad (2n)$$

The input impedance of the differential voltage multiplier is a function of the number of multiplication stages. According to the results of our simulation in ADS, the input impedance of the differential voltage multiplier decreases as the number of multiplication stage increases [15]. To maximize the energy harvesting efficiency, the number of multiplication stages can be chosen in a way to minimize the difference between the input impedance of the differential voltage multiplier and the characteristic impedance of the transmission medium.

IV. EXPERIMENTS

Two experiments have been conducted to explore the feasibility of wireless power transfer based on an RF plasma, with experiment I designed to prove the transmission of a plasma energy through water and experiment II designed to prove the transmission of a plasma energy through air.

The plasma source is an USB-compatible and battery-powered plasma ball. According to the manufacturer data sheet, the plasma source is an RF plasma consuming no

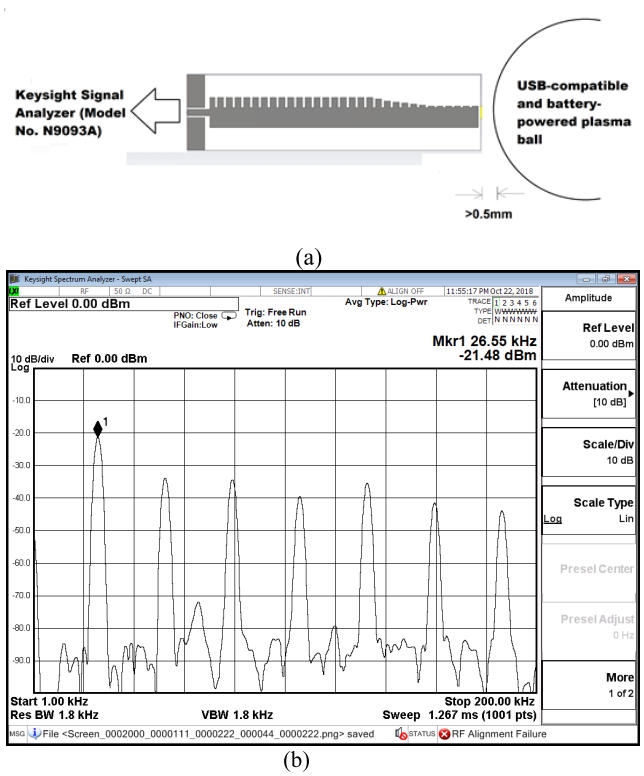

FIGURE 3. RF-plasma power source: a) Conducting measurement of the power of the RF plasma using an RF endfire antenna; b) Spectrum of the power at an observation point about 3cm from the RF plasma source (measured using Keysight Signal Analyzer N9030A).

more than 1 watt. We have measured the spectrum of the output power radiated from the plasma ball using an endfire antenna [23] as shown in Fig. 3(a), and Keysight Signal Analyzer (Model No. N9093A) (See Fig. 2). According to the spectrum as shown in Fig. 3(b), the fundamental frequency was 26.55 KHz and the corresponding power was −21.48 dB. The diameter of the plasma ball was about 3 inches. The endfire antenna was simulated using CST ^{TM} electromagentic simulator. By calculation of the simulated S-parameters of the endfire antenna, the available power gain of the antenna was determined to be −30 dB at 26.5 kHz. The loss of the cable is approximately 1 dB. By calculation using the data from the power spectrum, the loss of the antenna and the loss of the cable, the total plasma power available from the RF plasma source was determined to be approximately 0.02 watts.

A. EXPERIMENT I: WIRELESS POWER TRANSFER THROUGH WATER

Fig. 4(a) shows an experimental setup for wireless power transfer using an RF plasma wave. The bright line inside the plasma ball suggests that the majority of the RF plasma was being focused and transmitted through the monopole antenna which turns the energy from the RF plasma into a surface wave. The results of this experiment strongly suggest that this energy has somehow propagated along the surface of water in the form of surface waves and eventually reached the single

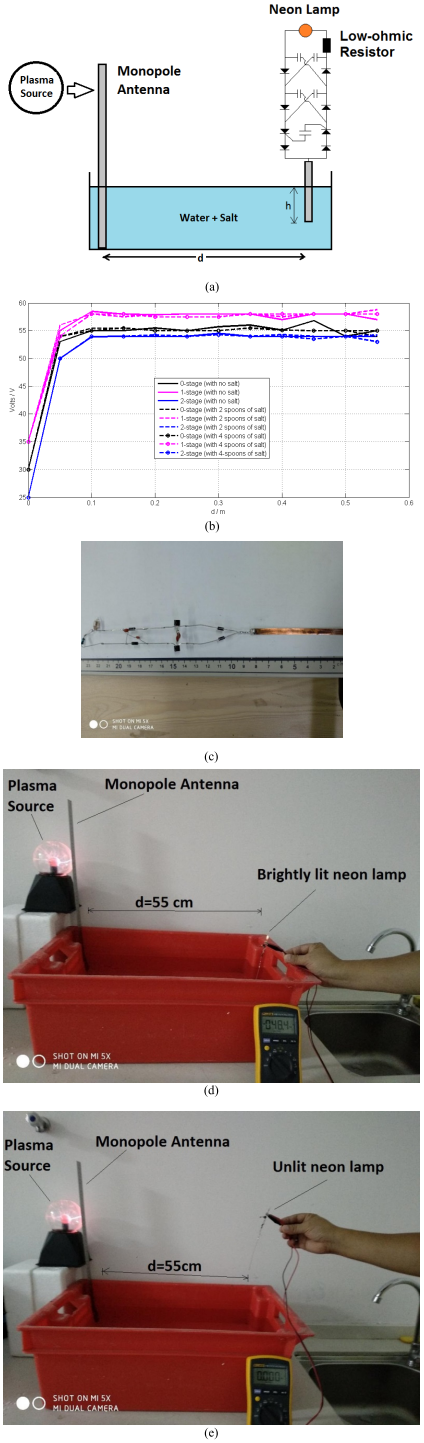

FIGURE 4. Experiment for wireless power transfer. a) the schematic view of the experimental setup; b) measured output voltage of the EHD as a function of distance between the transmitting and the receiving ends (Note: By measurement, the current in each case was about 0.3mA. *h* is approximately 10cm. *d* represents the distance between the monopole antenna at the transmitting end and the EHD. *Vout* stands for the voltage measured between the two terminals of the neon lamp. 0-stage means there was no differential voltage multiplier; 1-stage means there was 1 multiplication stage in the EHD; and 2-stage means there was 2 multiplication stage in the EHD); c) Photo of the EHD with one voltage multiplication stage (diodes used were 1N4001); d) The neon lamp was brightly lit when the single-wire input of the EHD was immersed in water to depth *h* (~3cm). e) The neon lamp became unlit when the single-wire input of the EHD was NOT immersed in water.

wire input port of the EHD at the receiving end. The output of EHD was terminated with a neon lamp (NE-2V), which requires at least 40 volts to light up.

The low-ohmic resistor connection in series with the neon lamp was intended for measurement of current. Let's say the resistance of this small resistor is *Rx*. The voltage of the neon lamp was determined by measuring the voltage across its terminals using different models of multimeters. The multimeters we have used include Fluke 17B Digital Multimeter and Fluke 17C Digital Multimeter. The voltage across the resistor (say *Vx*) was also measured. The current flowing through the neon lamp is determined by *Vx/Rx*.

The following values of *Rx* have been in our experiments for measurement of the current at the load (i.e. the neon lamp): 1 ohm, 4.7 ohm and 100 ohm. It is important to note that all the *Rx* values we have chosen are substantially less than the resistance of the neon lamp.

The output voltages were measured against the distance when the water was added with different amounts of salts.

Fig. 4(c) shows the photograph of an EHD which contains one multiplication stage. The diodes used in this circuit are 1N4001. The thyristor was MCR100-6. The circuit was implemented in the absence of any substrate due to concern that the substrate can potentially dampen the high order modes.

The experiment setup is illustrated in Figs. 4 (d) and (e). When the single-wire input of the EHD was immersed in water to a depth (approximately, $h = 30mm$), the neon lamp was brightly lit with the voltage across its terminals being greater than 50 volts (See Fig. 4(d)). The measured current was substantially higher than the calculated value. However, when the single-wire input of the EHD was away from water, the neon lamp was not lit (See Fig. 4(e)).

The measurement of this experiment are summarized in Fig. 4(b), where *d* represents the distance between the monopole antenna at the transmitting end and the EHD and *Vout* stands for the voltage measured between the two terminals of the neon lamp.

What follows is a list of observations about this experiment:

- In all cases, the neon lamp was brightly lit during the experiment.
- In general, when *h* was around 10mm, the measured output voltage was found to be highest at 58 volts when the number of multiplication stages at the EHD became 1. The current in this case was slightly above 0.3 mA, corresponding to an output power of 0.0174 watts at the load. By calculation on the measured data, the transmission efficiency was approximately 87%.
- The measured output voltage was found to be highest at 58 volts when the number of multiplication stages at the EHD became 1.
- The salt concentration in water did not appear to have any influence on the transmission efficiency.
- The output voltage *Vout* did not appear to be a strong function of the transmission range, *d*.
- The harvested energy at the output of the EHD has in general decreased and become dependent on the transmission range if the operating frequency of the source was increased to the MHz range.

On the other hand, when the power source was replaced with another plasma source power by household power supply, and the neon lamp was replaced with NE-2H, a maximum voltage of 65 volts was obtained. The current at the neon lamp was 3mA, corresponding to 0.195 watts.

B. EXPERIMENT II: ENERGIZING WEARABLE DEVICES THROUGH AIR

Fig. 5(a) shows an experimental setup demonstrating how to wirelessly power wear electronics. Here, the human body was used as a capacitor connected to an RF ground. The EHD was connected to neon lamp (NE-2) which was used as a wearable device inserted into the ear canal. The purpose of using a neon lamp instead of other devices was to demonstrate how much power could be realistically harvested.

As mentioned in the previous section, the low-ohmic resistor connected in series with the neon lamp was intended for measurement of current. Suppose the resistance of the low-ohmic resistor is *Rx*. In this case, the current through the neon lamp was the voltage across the low-ohmic resistor divided by *Rx*. Using this technique, we found that the current is in general 0.3 mA when the neon lamp was lit.

The single-wire transmission line at the input of the EHD was left open-circuited and used as a monopole antenna connected to the EHD was exposed to air. Each of the terminals of the neon lamp formed two capacitances connected to the body which is believed to be a source of negative charges. The EHD was remotely powered by an RF plasma source, of which the output power was less than 1 watt. The plasma energy was transmitted as a space wave through the space between the transmitting end and the receiving end.

Fig. 5(b) shows the output voltage of the energy harvesting device as a function of separation between the transmitting end and the receiving end. The neon lamp was brightly lit when the distance between the RF plasma source and the EHD was within 1.1 cm. According to the measured results, the energy harvesting device with one multiplication stage is most suitable for harvesting energy from a space wave.

When the transmission range is greater than 12 cm, the power density in the receiving end was found to be negatively associated with the transmission range. For each measurement, the measured output voltage was almost inversely proportional to distance. According to our measurements, the distance between the monopole antenna and the single-wire input of the EHD must be less than 12 cm in order to turn on the neon lamp (See Fig. 5(c)); otherwise, the neon lamp remain unlit (See Fig. 5(d)).

In addition to using the EHD's, we have also placed a bare neon lamp in vicinity of the plasma source to conduct a control experiment for Experiment II. The bare neon lamp was not attached to any energy harvesting circuit or fingers. It was dimly lit when its distance away from the plasma source is

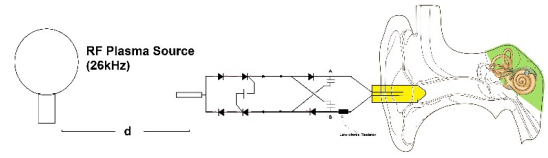

(a)

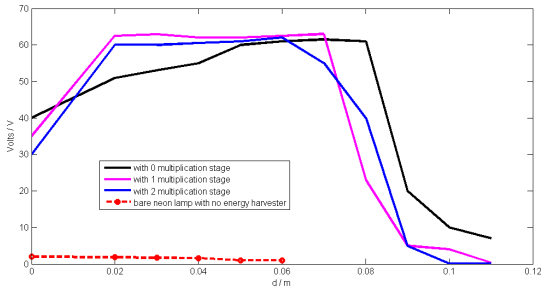

(b)

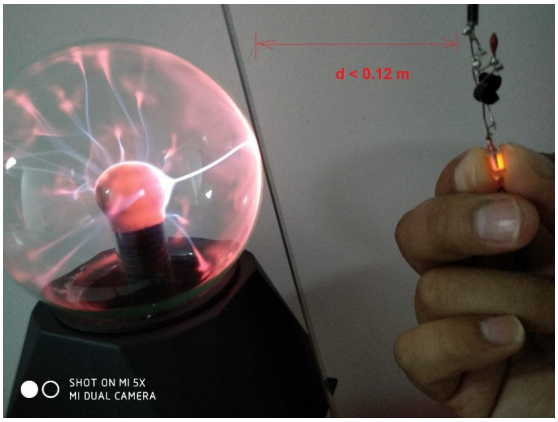

(c)

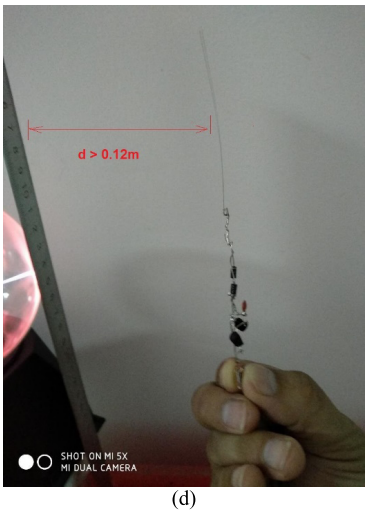

(d)

FIGURE 5. Energizing wearable electronics using the proposed energy harvesting device. a) Schematic diagram showing how a wearable device (as highlighted in yellow) is wirelessly powered. (In this experiment, a neon lamp was used as wearable device); and b) Measured output voltage of the energy harvesting device as a function of its distance from the plasma source. (*d* represents the distance between the monopole antenna at the transmitting end and the EHD. *Vout* stands for the voltage measured between the two terminals of the neon lamp; c) the neon lamp was lit when its distance from the monopole antenna was less than 12 cm; d) the neon lamp was not lit when its distance from the monopole antenna was more than 12 cm.

TABLE 1. Summarized findings of Experiment II.

	Maximum distance from the plasma source at which the neon lamp was lit (cm)	Estimated maximum power (W)
Bare neon lamp	<6	9.0000e-04
Neon lamp attached to the EHD with no multiplication stage.	<12	0.0183
Neon lamp attached to the EHD with 1 multiplication stage.	<12	0.0186
Neon lamp attached to the EHD with 2 multiplication stages.	<12	0.018

within 6cm. However, the voltage across the terminals of the bare neon lamp was at most 2 volts (See the red dashed curve in Fig. 5(b)). The findings of Experiment II are summarized in Table 1.

V. DISCUSSION

Our experiments were successfully replicated regardless if the RF plasma source was powered by a battery, a USB 2.0 port from a computer or a standard household electricity supply. According to the manufacturer, the RF plasma source requires a maximum power input of 1 watt to operate. At the time of this writing, the maximum power output from a USB 2.0 port is 2.5 watts. The results of both experiments have demonstrated the feasibility of wireless energy harvesting from an inexpensive USB/battery powered RF plasma source.

In Experiment I, where water was the transmission media, the operating frequency of the plasma was 26.6 KHz (or 167 rad/s), corresponding to a wavelength of 12km. The measurement of experiment I was obviously conducted within the near field zone. Perhaps, this explains why the transmission efficiency was virtually independent of the transmission range.

The plasmon frequency of water is known to be 21eV (or 8.6849×1015 Hz) [19]. According to the analysis given in Section II, the transmitted energy is primarily plasma surface wave, of which the electric field strength is highest in vicinity of the water surface. This clearly explains why the amount of salts added to the water has not significantly affected transmission efficiency in experiment I.

It is also possible to explain the phenomenon observed in experiment I using the known theory of lateral wave [12], [20], [21]. Ground wave is a superimposition of lateral waves, space waves and the trapped surface waves. Space waves are known to be independent of the conductivity of the transmission media. Laterals waves are weakly dependent on the conductivity of the transmission media. Trapped surface waves are the only component of a ground wave highly dependent on the conductivity of the transmission media. In this experiment, the weak dependency of the transmission efficiency on the conductivity of water is also

suggestive of lateral waves being involved as a dominant propagation mode. The result of experiment I also suggests that the dominant propagation mode of this RF plasma was unlikely a trapped surface wave.

In experiment II, the transmission efficiency of the space wave is noticeably low and is negatively associated with the transmission range. This result agrees with the conventional space wave theory in the sense that the power density is inversely proportional to the square of the distance between the transmitting end and the receiving end.

In experiment II, the energy harvesting device with one voltage multiplication stage has outperformed those with differential voltage multiplications. The phenomenon can be best explained in terms of impedance matching. The characteristic impedance of air is 377 ohm, which is relatively high compared to the characteristic impedance of a physical transmission medium. By our ADS simulation [15], the input impedance of the EHD decreases as the number of multiplication stages increases. The actual impedance of the EHD with one-stage multiplication perhaps matches more closely to 377 ohm.

Energising wear electronics is not the only goal of this work. The results of Experiment suggest that the EHD methodology can be used for sensing RF plasma. The RF plasma we used in our experiment is not much different from the RF plasma being used in a Plasma Enhanced Chemical Vapor Deposition chamber (PECVD) for coating epitaxial layer onto a dielectric wafer. The secondary RF plasma in a PECVD normally operates at RF frequencies below 500 KHz. Battery-powered devices should not be placed inside the PECVD chamber because this will directly cause contamination. The results of Experiment II have proven that our single-wire can be used to detect an ambient RF power in the absence of any power supply. In addition, according to the circuit as shown in Fig. 2a, *Cg* allows AC current to pass through without interfering other parts of the circuit. Whilst the load at the EHD can reveal the detected power, the frequency of the AC voltage at *Cg* can be used to calculate fundamental frequency of the detected RF plasma without a spectrum analyser or a network analyser. The same EHD methodology can be applied in other systems which require a detection of RF plasmas.

The authors strongly believe that the results of this investigation has a much wider implications in terms of the future of the renewable energy industry. Overall speaking, the findings from both experiments have opened up not only the possibility of energizing wearable electronics with an RF plasma or sensing an RF plasma, but also the feasibility of harvesting energy from a natural plasma source such as the lightning strikes from the sky. Although the electric plasma used in this investigation is nowhere close to a lightning strike in nature in terms of the power level, the findings of experiment I strongly suggest that the energy from lightning strikes on oceans or wet lands can be harvested as a plasma surface wave and stored in the form of a DC electricity. With some creativity, the scenario of Experiment I can be further extended

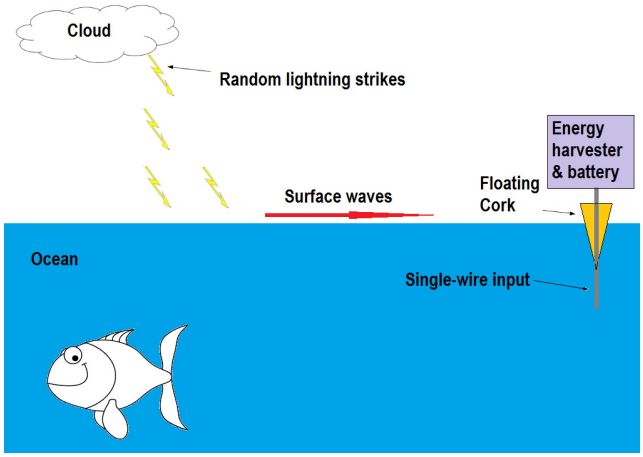

(a)

(b)

FIGURE 6. Harvesting lightning energy from an ocean. a) Proposed technique for harvesting lightning on an ocean. b) The frequent lightning phenomena in Catatumbo River.

to capture a plasma surface energy from random lightning strikes in a manner similar to what is illustrated in Fig. 6a. In Fig. 6a, the energy harvester is supported by a floating cork which is attached to a straight single wire immersed in the sea water. The energy harvester can be unmanned but its location should be remotely identifiable and controllable. To maximize the amount of harvested energy, multiple floating energy harvesters, such as the one illustrated in Fig. 6a, can be used.

Being able to harvesting lightning energy can potentially shift the paradigm of the global economy. In some areas such as Lake Maracaibo and the Catatumbo River in Venezuela as shown in Fig. 6b, lightning events occur at the rate of about 28 strikes per minute [10]. The same region experiences 1.2 million lighting strikes a year [10]. A single lightning strike carries about five billion Joules of energy on average [9]. By estimation, this region receives approximately 6,000 trillion joules per year. Other similar hotspots of lightning include The Democratic Republic of the Congo, Caceres in Colombia, El Tarra in Colombia, Daggar in Pakistan, Northwestern South America, The Himalayan Forelands, Central Florida, The Pampas of Argentina as well as Indonesia [11].

VI. CONCLUSION

In this work, two experiments have been conducted to demonstrate how an RF plasma can be remotely transmitted with no ground return and harvested as a storable DC voltage.

In experiment I, the RF plasma was transmitted through a tank of ungrounded water and harvested as a DC voltage at the receiving end using a device equipped with an Avramenko diode configuration and a differential voltage multiplier. As a result of experiment I, we concluded the following observations: 1) the harvested power was in general strong enough at least to light up an neon lamp; 2) the actual power harvested was highly dependent on the number of multiplication stages in the differential multiplier; 3) the measured transmission efficiency does not appear to be a strong function of the transmission range or the water conductivity; and 4) the RF plasma has been transmitted as a plasma surface wave.

In experiment II, the plasma energy was transmitted through air and harvested using the same energy harvesting device. The harvesting efficiency was stable over a limited range, beyond which the plasma energy was found to be deliverable through air at the expense of transmission efficiency. According to the measured results, the energy harvesting device with one multiplication stage is most suitable for harvesting energy from a space wave.

Overall speaking, the findings of this work have opened up the possibility for energizing wearable electronics with an RF plasma, for sensing an RF-plasma and for harvesting the energy of a natural plasma source.

ACKNOWLEDGMENT

Louis W. Liu, Abhishek Kandwal, Hongjian Shi, and Qingsha S. Cheng contributed equally to this work.

REFERENCES

[1] S. Jacobs. (Aug. 2014). Wireless power for minuscule medical implants. MIT Technology Review. Accessed: Aug. 14, 2018. [Online]. Available: https://www.technologyreview.com/s/530006/wireless-power-for-minuscule-medical-implants

[2] A. Abid *et al.*, "Wireless power transfer to millimeter-sized gastrointestinal electronics validated in a swine model," *Sci. Rep.*, vol. 7, Apr. 2017, Art. no. 46745, doi: 10.1038/srep46745.

[3] N. Tesla, "Light and other high-frequency phenomena," Franklin Inst., Philadelphia, PA, USA, Tech. Rep., 1893.

[4] N. Tesla, *The Problem of Increasing Human Energy: With Special Reference to the Harnessing of the Sun's Energy*. Century Magazine, Jun. 1900.

[5] G. Marconi, "Wireless telegraphic communication: Nobel lecture," Nobel Lectures Physics, no. 196-222, 1996, p. 206.

[6] Electrical Engineering Stack Exchange. (Mar. 2015). *Is 20 Watts of Electricity Dangerous?* [Online]. Available: https://electronics.stackexchange.com/questions/158603/is-20-watts-of-electricity-dangerous/158610#158610

[7] J. Abaygar. (Jun. 2015). How will my body react to very high frequency currents, considering skin effects? Quora. [Online]. Available: https://www.quora.com/How-will-my-body-react-to-very-high-frequency-currents-considering-skin-effects

[8] Institute Physics Staff. *A Bolt of Lightning has Enough Energy to Toast 100,000 Slices of Bread*. Accessed: Sep. 7, 2018. [Online]. Available: http://www.physics.org/facts/toast-power.asp

[9] BBC Staff. (Jul. 28, 2014). Who, what, why: What happens when lightning hits the sea? Magazine Monitor. Accessed: Sep. 7, 2018. [Online]. Available: https://www.bbc.com/news/blogs-magazine-monitor-28521789

[10] O. S. Nag. (Apr. 25, 2017). What is catatumbo lightning? Environment, World Atlas. Accessed: Sep. 7, 2018. [Online]. Available: https://www.worldatlas.com/articles/what-is-catatumbo-lightning.html

[11] R. I. Albrecht, S. J. Goodman, D. E. Buechler, R. J. Blakeslee, and H. J. Christian, "Where are the lightning hotspots on Earth?" *Bull. Amer. Meteorol. Soc.*, May 2016, doi: 10.1175/BAMS-D-14-00193.1.

[12] L. W. Y. Liu, A. Kandwal, Z. E. Eremenko, and Q. Zhang, "Open-ended voltage multipliers for wireless transmission of electric power," *J. Microw. Power Electromagn. Energy*, vol. 51, no. 3, pp. 187–204, 2017.

[13] L. W. Y. Liu, S. Ge, Q. Zhang, and Y. Chen, "Capturing surface electromagnetic energy into a DC through single-conductor transmission line at microwave frequencies," *Prog. Electromagn. Res. M*, vol. 54, pp. 29–36, 2017.

[14] L. W. Y. Liu, Q. Zhang, Y. Chen, M. A. Teeti, and R. Das, "Wireless energy harvesting by direct voltage multiplication on lateral waves from a suspended dielectric layer," *IEEE Access*, vol. 5, pp. 21873–21884, Sep. 2017, doi: 10.1109/ACCESS.2017.2757947.2017.

[15] L. W. Y. Liu, Q. Zhang, and Y. Chen, "Avramenko diode circuit topology for microwave energy harvesting in Goubau line and wireless mediums," *IEEE Access*, vol. 6, pp. 18883–18893, Apr. 2018, doi: 10.1109/ACCESS.2018.2822342.

[16] C. S. Liu and Y. K. Tripathi, *Electromagnetic Theory for Telecommunications*. Cambridge, U.K.: Cambridge Univ. Press, 2007.

[17] J. A. LaVerne and A. Mozumder, "Concerning plasmon excitation in liquid water," *Radiat. Res.*, vol. 133, no. 3, pp. 282–288, 1993.

[18] R. E. Collin, "Some observations about the near zone electric field of a Hertzian dipole above a lossy earth," *IEEE Trans. Antennas Propag.*, vol. 52, no. 11, pp. 3133–3137, Nov. 2004.

[19] R. E. Collin, "Hertzian dipole radiating over a lossy earth or sea: Some early and late 20th-century controversies," *IEEE Antennas Propag. Mag.*, vol. 46, no. 2, pp. 64–79, Apr. 2004.

[20] J. D. Cross and P. R. Atkins, "Electromagnetic propagation in four-layered media due to a vertical electric dipole: A clarification," *IEEE Trans. Antennas Propag.*, vol. 63, no. 2, pp. 866–870, Feb. 2015.

[21] R. King, M. Owens, and T. T. Wu, *Lateral Electromagnetic Waves*. Springer-Verlag, 1992.

[22] T. Tamir, "Experimental verification of a lateral wave above a lossy interface," *Electron. Lett.*, vol. 6, no. 12, pp. 357–358, Jun. 1970.

[23] T. Tamir and T. D. Staiman, "Nature and optimization of ground wave excited by submerged antennas," *Proc. IEE*, vol. 113, no. 8, pp. 1299–1310, 1986.

[24] A. Kandwal, Q. Zhang, X.-L. Tang, L. W. Liu, and G. Zhang, "Low-profile spoof surface plasmon polaritons traveling-wave antenna for near-endfire radiation," *IEEE Antenna Wireless Propag. Lett.*, vol. 17, no. 2, pp. 184–187, Feb. 2018.

[25] N. E. Zaev, S. V. Avramnko, and L. V. Lisin, "Conduction current test, activated by polarization current," *Magazine Russian Phys. Thought*, 1991

Authors' photographs and biographies not available at the time of publication.